# Associative Behavior-Based abundance Index (ABBI) for western Indian Ocean skipjack tuna (*Katsuwonus pelamis*) obtained from echosounder buoys data.

Yannick Baidai[1], Amaël Dupaix[2], Antoine Duparc[2], Laurent Dagorn[2], Jean-Louis Deneubourg[3], and Manuela Capello[2]

## ABSTRACT

This paper presents the abundance estimates of skipjack tuna (*Katsuwonus pelamis*) using the Associative Behavior-Based abundance Index (ABBI). By taking advantage of the associative behavior of species around floating objects (FOBs) and acoustic data collected by echosounder buoys used in the tropical tuna purse seine fishery, the ABBI approach provides direct and effort-independent estimates of tropical tuna abundance. Its implementation in the western Indian Ocean for skipjack has shown that the decline in abundance of this species observed since 2018 is shifting towards a stabilization trend of abundance around 2013 levels from 2020 onwards.

**Keywords**: *Abundance Index; Associative behavior; FADs; Skipjack tuna*

## 1. INTRODUCTION

Defined as man-made floating objects, specifically designed to attract and concentrate tunas, DFADs are typically equipped with tracking technology (GPS) and echosounder buoys to remotely detect the associated tuna biomass and their location (Lopez *et al.*, 2014). DFADs have considerably increased the catchability of tropical tuna species, notably skipjack tuna, and are considered as one of the most important changes that have contributed to the increase in the efficiency of purse seiners (Fonteneau *et al.*, 2013). However, the non-random nature of this fishing method has significantly complicated the estimation of fishing effort in the purse seine fishery and, consequently, the standardization of CPUE abundance indices from purse-seine catches obtained of tropical tuna associated with DFADs.

Recently, the availability to scientists of new data obtained from electronic tagging and/or echosounder buoys has allowed the development of alternative methods for deriving abundance

[1] African Marine Expertises, Abidjan, Côte d'Ivoire
[2] MARBEC, Univ Montpellier, CNRS, Ifremer, IRD, Sète, France
[3] Unit of Social Ecology, Université Libre de Bruxelles (ULB), Bruxelles, Belgium

indices for tropical tuna populations (Capello *et al.*, 2016; Santiago *et al.*, 2020; Baidai *et al.*, 2021). Within this perspective, this work addresses the population assessment of skipjack tuna in the western Indian Ocean, based on a dedicated methodology which exploits the associative behavior of this species, quantified using data from echosounder buoys attached to DFADs and electronic tagging experiments, in order to derive direct and effort-independent abundance estimates: the Associative Behavior-Based abundance Index (ABBI).

## 2. MATERIALS AND METHODS

### *2.1. Model definition*

Due to their associative behaviour, the total abundance of tropical tunas ($N$), calculated at a given time (t) in a given area, results from the sum of the two components of their population: the associated one ($X_a$), *i.e.* the tuna schools associated with floating objects, and the unassociated one, *i.e.* free-swimming schools of tunas ($X_u$).

$$N(t) = X_a(t) + X_u(t) \tag{1}$$

Within a given study region and time period, the average associated tuna population ($\widehat{X_a}$) can be estimated as follows:

$$\widehat{X_a} = \hat{m}\hat{f}\hat{p} \tag{2}$$

Where $\hat{m}$ is the average tuna biomass estimated under FOBs occupied by tuna aggregation, $\hat{f}$ represents the average proportion of FOBs with tuna aggregations and $\hat{p}$ the average number of FOBs in the region of interest.

Capello *et al.*, (2016) demonstrated that the ratio between the average size of the associated component to the total population can be estimated by measuring the uninterrupted period of time that tunas spend either associated with, or disassociated from a FOB, *i.e.,* the average continuous residence time (CRT) and the average continuous absence time (CAT):

$$\frac{\widehat{X_a}}{\widehat{N}} = \frac{CRT}{CRT + CAT} \tag{3}$$

Considering Equations (2-3), the total tuna population within an area can be estimated as:

$$\widehat{N} = \hat{m}\hat{f}\hat{p}\left(1 + \frac{CAT}{CRT}\right) \tag{4}$$

Furthermore, considering Equations (1 – 2) and (4), the free-swimming population ($X_u$) can be expressed from the following relation:

$$\widehat{X_u} = \frac{CAT}{CRT}\widehat{m}\widehat{f}\widehat{p} \tag{5}$$

### 2.2. *Study area and period*

The study area extended over the western Indian Ocean, between latitudes 10° S and 10° N and covered longitudes located between the eastern African coasts and 70° E (Figure 1). The abundance estimates were conducted in between 2013 and 2019, using a spatio-temporal stratification of 10°×10° and quarter-year (Figure 1).

### 2.3. *Field data*

#### *2.3.1. Estimated number of floating objects ($\hat{p}$)*

The estimation of the number of FOBs in each of the time-area units followed two different approaches. From 2013 to 2019, it was assessed from the number of buoys equipping the DFADs deployed by the French tuna purse seine fleet ($n_{french\ buoys}$), and two raising factors. The ratio between DFADs deployed by French and Spanish purse-seiners fleets ($R_1$), provided from 2010 to the end of 2017, by Katara *et al.* (2018), allowed estimates of the total number of DFADs. The missing ratios for the 2018 and 2019 were estimated using the average ratio over the year 2017, based on the assumption of a relative stabilization in the exploitation of buoys between the different fleets after this period (limitation measures on the number of buoys operated by tuna purse-seiners in the Indian Ocean: IOTC Resolutions 15/08 and 17/08).
The total number of FOBs in each strata was then derived from the ratios $R_2$ of DFADs encountered by observers on-board French tuna seiners, relative to other floating objects (referred herein as LOGs) consisting of natural (marine mammals, trees, etc.) or artificial (debris from human activities) floating objects found in the open ocean that are not constructed/deployed by tuna fishers (Figure 2A).

$$\hat{p}_{[2013-2019]} = n_{french\ buoys}(1 + R_1)(1 + R_2) \tag{6}$$

This ratio was derived from observers' data collected through the Data Collection Framework (Reg 2017/1004 and 2016/1251) funded by both IRD and the European Union since 2005, and OCUP ("Observateur Commun Unique et Permanent"), an industry-funded program coordinated by ORTHONGEL since 2014, with an overall average coverage rate of about 50%

over the years 2013 to 2017 (Goujon *et al.*, 2017). The observer data include the date, time, and location of the main activities of the vessel (e.g. fishing sets, installation or modification of FOBs, and searching for FOBs). For every activity occurring on a FOB, the type of operation (e.g. deployment, removal, and observation of a FOB) and the type of object (DFAD or LOG) are reported.

From 2020 to 2021, the estimation of FOBs number have benefited from the recent availability of buoy data from tuna purse-seine vessels provided by the IOTC Secretariat (IOTC, 2022). This dataset consist of the monthly mean of the number of operational buoys for each 1°×1° cell of the Indian Ocean, used as a proxy for DFAD number. DFAD number were summed over 10° cells and averaged to the quarter-year temporal resolution. FOB numbers were calculated using DFAD number and data recorded by scientific observers onboard French purse seine vessels (2014-2019). Using observers data, and the methodology developed in Dupaix *et al.* (2021), we calculated a mean monthly ratio ($R_3$):

$$R_3 = \frac{n_{LOG}}{n_{DFAD}} \quad (7)$$

with $n_{LOG}$ and $n_{DFAD}$ the number of LOG and DFAD observations respectively. The ratio was then used to calculated the number of FOBS per 10° cell which was used to calculate the number of FOBs over 2020-2021 as follows:

$$\hat{p}_{[2020-2021]} = n_{DFAD}(1 + R_3) \quad (8)$$

Figure 2B shows the time series of the estimated number of FOBs in the different spatial strata considered in the study area.

### *2.3.2. FOB-associated average tuna biomass ($\hat{m}$)*

The average biomasses of skipjack (size category under 10 kg) around a FOB were derived from purse seine catch-per-set data reported in the vessel logbooks of the French fleet (Table 1). FOB-associated catches-per-set reported in vessel logbooks were corrected using a dedicated procedure referred to as levels 1 and 2 of the T3 processing (Bach *et al.*, 2018; Duparc *et al.*, 2018; Depetris and Lebranchu, 2020). Level 1 adjusts the catch-per-set values declared in vessel logbooks using landing notes, to improve the accuracy of catch estimates provided by skippers. Level 2 estimates the species and size compositions of FOB sets based on port sampling data

Since landing notes were available for all fishing trips, Level 1 was applied to correct the reported catch-per-set of all FOB sets recorded in vessel logbook data. Level 2, on the other hand, was applied only to the FOB sets conducted during the fishing trips that were sampled at landing. These FOB sets are referred to as "sampled FOB sets".

Species compositions (i.e., percentages of catches by species and size category in the sampled FOB sets) were averaged by stratum, with a minimum threshold of 20 available sampled sets per strata. Where species composition values were missing for a given stratum, they were generated using their corresponding estimated marginal means (aka least-squares means), in a reference grid as described by Lenth (2016). The reference grid consists of the set of all combinations of predictor levels (i.e. the time-area strata) and estimated marginal means were the prediction values from the species composition models. We assessed the species composition of sets using a zero-one-inflated Beta regression model, in which the likelihood was fitted with frequentist inference (Rigby *et al.*, 2019). An equal weight of one were used for all observations, assuming representativeness in each stratum considering the sample size. The proportion of the target species in the set obtained from the sampling programs formed the response variable, while the year, quarter and spatial strata were predictors. All predictors were used to model the mean, variance, zero-inflated and one-inflated components of the model. Model selections were performed on each model component using a Generalized Akaike Information Criterion. Diagnostics of the selected models were checked: the normalized quantile residuals against the fitted values and the case number (i.e. index number), together with their kernel density estimate and a normal Q-Q plot (Figure 3a).

Finally, the average biomasses of skipjack associated with a FOB ($\widehat{m}$) were calculated for each stratum by multiplying the average catch-per-set of all FOBs (including both sampled and not-sampled sets, all adjusted through the level 1 of the T3 processing) by the average species composition. Only the strata with at least 20 FOB sets (including both sampled and not-sampled sets) were considered.

The catch and species composition data provided by the Ob7 were collected under the Data Collection Framework (Reg. 2017/1004 and 2016/1251) funded by IRD and the European Union. The figure 4 provides the time series of the FOB-associated biomasses obtained from this protocol, for each of the three species, across the various spatial strata considered.

### *2.3.3. Proportion of inhabited FOBs ($\hat{f}$)*

Acoustic data collected by the Marine Instruments M3I buoys were translated into presence/absence of a tuna aggregation, using a machine learning algorithm (Baidai *et al.*, 2020), that was shown to provide good accuracies (85%) in the Indian Ocean. The first sections of presence or absence occurring at the beginning of the FAD trajectories were excluded from the analysis as they may result from the colonization period of the DFAD during which the DFAD-tuna system is not yet at equilibrium, or potentially from classification errors related to the operation on the buoy (Baidai *et al.,* 2020).

Daily presence/absence data were then used to derive the proportion of FOBs inhabited by a tuna aggregation ($f$). This was expressed as the number of DFADs (equipped by an M3I buoy) classified as inhabited by a tuna aggregation, divided by the total number of M3I buoys at a daily scale. A threshold of at least 10 available buoys per day and space-time unit was considered for the calculation of the daily proportion of inhabited FOBs. Table 1 provides the average daily numbers of available M3I buoys used over the study area. Quarterly averages of the proportion of inhabited FOBs were then calculated. Because an accurate species discrimination from these acoustic data was not possible, these values were corrected with the occurrence of skipjack tuna in the FOB-associated tuna aggregations, according to Equation (6):

$$f(SKJ) = f\eta(SKJ) \tag{9}$$

where $\eta(SKJ)$ represents the ratio between the number of DFAD-catches with a biomass of skipjack tuna relative to the total number of positive DFAD catches (considering only DFAD catches with a total biomass greater than or equal to 1 tonne).. This ratio was estimated on a quarterly basis, within each grid cell, using the sampling data raised to the catch per set. A minimum number of 20 available sampling data per strata was considered for the ratio calculation. Missing occurrence values for a given stratum were estimated from a binomial model using year, quarter and spatial strata as predictors (Figure 3b). The time series of the estimated proportions of FOBs inhabited by skipjack tuna are presented in the figure 5.

### *2.3.4. Continuous residence time of skipjack tuna (CRT)*

Tuna CRTs have been shown to vary according to their species, size (Ohta et Kakuma, 2005; Robert *et al.*, 2012, Rodriguez et al. 2017) and FOB density (Pérez *et al.*, 2020). Nevertheless, numerous studies across all tropical oceans have shown that the magnitude of these variations remains relatively small for the three tuna species and the life stages considered in this work (Dagorn *et al.*, 2007; Matsumoto *et al.*, 2014, 2016; Tolotti *et al.*, 2020; Govinden *et al.*, 2021). Considering this characteristic, a constant CRT value was assumed for skipjack tuna in all spatial and temporal strata. The value was provided by Govinden et *al.* (2021), who measured an average CRT at DFADs for skipjack tunas of 4.58 ± 4.78 days.

### *2.3.5. Continuous absence time of skipjack tuna (CAT)*

At the time of the study, only CRTs were experimentally measured for the three species on DFADs. However, acoustic tagging experiments conducted in arrays of anchored Fish Aggregating Devices (AFADs) showed that CATs decrease for decreasing distances among AFADs, due to an increased AFAD encounter rate by tuna at higher AFAD densities (Pérez *et al.*, 2020). Based on these findings, the following Ansatz relating the average CAT to the number of FOBs ($\hat{p}$) was used:

$$CAT = \frac{1}{\phi\hat{p}} \qquad (10)$$

where $\phi$ is a parameter that depends on the probability of associating to one of the estimated $\hat{p}$ FOBs. To assess the sensitivity of the ABBI to $\phi$ values, a range of 2e-05 and 6e-05 that produces CAT values consistent with the findings from acoustic tagging studies (Robert *et al.*, 2013; Rodriguez-Tress *et al.*, 2017; Pérez *et al.*, 2020) and total catches in the study area, was considered for the abundance assessments.

## ***2.4. Abundance estimates***

Abundance estimates were conducted considering a spatio-temporal stratification of 10°/ quarter. In each 10°×10° grid cell, the associated, free-swimming and total skipjack abundance was calculated following respectively the Equations (2), (5) and (4). An average quarterly index was then estimated for the whole study area, considering the average over the spatial strata with available data for the same period, for each population components. Relative abundance indices for the different components are also provided, using the first quarter of the year 2013 (the first year with available data) as reference and different values of $\phi$ (for the total population).

## 3. Results and Discussion

### *3.1. Time series of abundance of skipjack tuna in the western Indian Ocean*

Figures 6, 7 and 8 show the abundance estimates per 10°/quarter of the associated, free-swimming and total skipjack tuna populations, respectively. Figure 9 presents the quarterly average estimates, calculated over the whole study area, of the absolute and relative abundance of the total skipjack population and its associated and free-swimming components. They reveal that globally both components of the skipjack population follow roughly similar trajectories throughout the study period. The result also highlighted a gradual decline in the abundance of skipjack tuna since 2018, stabilizing around the 2013 reference levels onwards 2020.

The variation of the $\phi$ values used for the free-swimming and the total population did not change the trends of the estimated biomass qualitatively. Indeed, when examined in relative terms, the ABBI showed very low sensitivity to the values of the parameter ($\phi$) used in setting the ranges of CAT. However, the variability of the absolute ABBI estimates remained closely linked to the ranges of CAT used.

From a set of descriptive metrics of the associative behaviour of tunas around floating objects (namely residence and absence times) and the occupancy rate of these objects by tuna aggregations, the ABBI approach thus provided direct, effort-independent and absolute abundance indices for skipjack tuna in the Western Indian Ocean. However, data collection remain one of the main challenges hindering its implementation. For instance, current collection of tuna continuous residence times (CRT) is usually related to short-term projects, and remains limited to specific oceanic regions and periods. Similarly, although technological means exist to measure the continuous absence time (CAT) of tuna, there are still several technical and logistical challenges to overcome before it can be consistently assessed over the large oceanic scales covered by DFADs (Dagorn *et al.*, 2007; Robert *et al.*, 2012, 2013; Rodriguez-Tress *et al.*, 2017). Additional efforts for regular and large-scale electronic tagging programs would be critical to provide a better understanding of the associative behavior of tunas, and to carry out accurate assessments of their populations based on the ABBI methodology.

Here the ABBI framework illustrates the important contribution that unconventional data sources and technologies such as electronic tagging and echosounder buoys can make towards improving the inputs in fish stock assessments. To date, the data required for this approach are mainly devoted to either improve general knowledge on the ecology of tuna species (behavioural metrics) or for commercial (acoustic monitoring of FADs deployed by purse seiners) or regulatory purposes (monitoring the number of FADs by regional fisheries management organizations). The possibility to derive abundance indices from these data using alternative approaches to CPUE-based methods could support future developments of dedicated data collection programs, and help improve tropical tuna stock assessments, and thus fisheries management.

## ACKNOWLEDGEMENTS

This project was co-funded by the ANR project BLUEMED (ANR-14-ACHN-0002) and "Observatoire des Ecosystèmes Pélagiques Tropicaux exploités" (Ob7) from IRD/MARBEC. The authors would also like to thank ISSF for supporting the project. The authors are grateful to ORTHONGEL and its contracting parties (CFTO, SAPMER, SAUPIQUET) for providing the echosounder buoys data. The authors sincerely thank the contribution of the staff of the Ob7 on the databases of the echosounder buoys. We are also deeply grateful to the buoy manufacturers for their useful advice and information on their echosounder buoys.

## REFERENCES

Bach, P., Cauquil, P., Depetris, M., Duparc, A., Floch, L., Lebranchu, J., and Sabarros, P. 2018. Procédures d'échantillonnage des thonidés tropicaux débarqués par les senneurs dans les océans Atlantique et Indien. ird-02132072. 70p pp. https://hal.ird.fr/ird-02132072.

Baidai, Y., Dagorn, L., Amande, M. J., Gaertner, D., and Capello, M. 2020. Machine learning for characterizing tropical tuna aggregations under Drifting Fish Aggregating Devices (DFADs) from commercial echosounder buoys data. Fisheries Research, 229: 105613. Elsevier. https://doi.org/10.1016/j.fishres.2020.105613.

Baidai, Y., Laurent, D., Gaertner, D., Deneubourg, J. L., Duparc, A., Floch, L., and Capello, M. 2021. Associative Behavior-Based abundance Index (ABBI) for yellowfin tuna (Thunnus albacares) in the Western Indian Ocean. 23th Working Party on Tropical Tuna, IOTC-2021-WPTT23(DP)-15_Rev1. 29 pp.

Capello, M., Deneubourg, J. L., Robert, M., Holland, K. N., Schaefer, K. M., and Dagorn, L. 2016. Population assessment of tropical tuna based on their associative behavior around floating objects. Scientific Reports, 6: 36415. The Author(s). https://www.nature.com/articles/srep36415#supplementary-information.

Dagorn, L., Pincock, D., Girard, C., Holland, K., Taquet, M., Sancho, G., Itano, D., *et al.* 2007. Satellite-linked acoustic receivers to observe behavior of fish in remote areas. Aquatic Living Resources, 20: 307–312. http://www.alr-journal.org/10.1051/alr:2008001.

Depetris, M., and Lebranchu, J. 2020. OB7-IRD/t3: Beta version of T3 software (Version

0.9.0).

Dupaix, A., Capello, M., Lett, C., Andrello, M., Barrier, N., Viennois, G., and Dagorn, L. 2021. Surface habitat modification through industrial tuna fishery practices. ICES Journal of Marine Science, 78: 3075–3088. Oxford University Press. https://academic.oup.com/icesjms/article/78/9/3075/6368416.

Duparc, A., Cauquil, P., Depetris, M., Dewals, P., Floch, L., Gaertner, D., Hervé, A., *et al.* 2018. Assessment of accuracy in processing purse seine tropical tuna catches with the T3 methodology using French fleet data. Working Party on Tropical Tunas (WPTT), IOTC-2018-WPTT20-16 Assessment. 19p pp. https://www.iotc.org/sites/default/files/documents/2018/10/IOTC-2018-WPTT20-16_Rev1.pdf.

Fonteneau, A., Chassot, E., and Bodin, N. 2013. Global spatio-temporal patterns in tropical tuna purse seine fisheries on drifting fish aggregating devices (DFADs): Taking a historical perspective to inform current challenges. Aquatic Living Resources, 26: 37–48. EDP Sciences. http://www.alr-journal.org/action/article_S0990744013000466%5Cnhttp://journals.cambridge.org/action/displayAbstract?fromPage=online&aid=8897405&fileId=S0990744013000466%5Cnhttp://journals.cambridge.org/action/displayFulltext?type=1&fid=8897410&jid=ALR&vol.

Goujon, M., Maufroy, A., Relot-Stirnemann, A., Moëc, E., Bach, P., Cauquil, P., and Sabarros, P. 2017. Collecting data on board French and Italian tropical tuna purse seiners with common observers: results of ORTHONGEL'S voluntary observer program OCUP (2013-2017) in the Indian ocean. IOTC-2017-WPDCS13-22_Rev1. 22 pp. https://www.iotc.org/sites/default/files/documents/2017/11/IOTC-2017-WPDCS13-22_Rev1_-_OBS_PS_FRA.pdf.

Govinden, R., Capello, M., Forget, F., Filmalter, J. D., and Dagorn, L. 2021. Behavior of skipjack (Katsuwonus pelamis), yellowfin (Thunnus albacares), and bigeye (T. obsesus) tunas associated with drifting fish aggregating devices (dFADs) in the Indian Ocean, assessed through acoustic telemetry. Fisheries Oceanography: fog.12536. https://onlinelibrary.wiley.com/doi/10.1111/fog.12536.

IOTC. 2022. Instrumented buoy data (Jan 2020—June 2022). IOTC ad hoc Working Group on FADs (WGFAD3). https://iotc.org/WGFAD/03/Data/04-BU.

Katara, I., Gaertner, D., Marsac, F., Grande, M., Kaplan, D., Agurtzane, U., Loreleï, G., *et al.* 2018. Standardisation of yellowfin tuna CPUE for the EU purse seine fleet operating in the Indian Ocean. 20th session of the Working Party on Tropical Tuna., IOTC–2018–WPTT20–36_Rev1. 1–14 pp. https://www.iotc.org/sites/default/files/documents/2018/10/IOTC-2018-WPTT20-36_Rev1.pdf.

Lenth, R. V. 2016. Least-Squares Means: The R Package lsmeans. Journal of Statistical Software, 69. http://www.jstatsoft.org/v69/i01/.

Lopez, J., Moreno, G., Sancristobal, I., and Murua, J. 2014. Evolution and current state of the technology of echo-sounder buoys used by Spanish tropical tuna purse seiners in the Atlantic, Indian and Pacific Oceans. Fisheries Research, 155: 127–137. http://dx.doi.org/10.1016/j.fishres.2014.02.033.

Matsumoto, T., Satoh, K., and Toyonaga, M. 2014. Behavior of skipjack tuna (Katsuwonus pelamis) associated with a drifting FAD monitored with ultrasonic transmitters in the equatorial central Pacific Ocean. Fisheries Research, 157: 78–85. Elsevier B.V. http://dx.doi.org/10.1016/j.fishres.2014.03.023.

Matsumoto, T., Satoh, K., Semba, Y., and Toyonaga, M. 2016. Comparison of the behavior of skipjack (Katsuwonus pelamis), yellowfin (Thunnus albacares) and bigeye (T. obesus) tuna associated with drifting FADs in the equatorial central Pacific Ocean. Fisheries Oceanography, 25: 565–581. http://doi.wiley.com/10.1111/fog.12173.

Ohta, I., and Kakuma, S. 2005. Periodic behavior and residence time of yellowfin and bigeye tuna associated with fish aggregating devices around Okinawa Islands, as identified with automated listening stations. Marine Biology, 146: 581–594. http://link.springer.com/10.1007/s00227-004-1456-x.

Pérez, G., Dagorn, L., Deneubourg, J. L., Forget, F., Filmalter, J. D., Holland, K., Itano, D., *et al.* 2020. Effects of habitat modifications on the movement behavior of animals: the case study of Fish Aggregating Devices (FADs) and tropical tunas. Movement Ecology, 8: 1–11. Movement Ecology.

Rigby, R., Stasinopoulos, M., Heller, G., and De Bastiani, F. 2019. Distributions for Modelling Location, Scale and Shape: Using GAMLSS in R. CRC Press. http://www.gamlss.com/wp-content/uploads/2018/01/DistributionsForModellingLocationScaleandShape.pdf.

Robert, M., Dagorn, L., Deneubourg, J. L., Itano, D., and Holland, K. 2012. Size-dependent behavior of tuna in an array of fish aggregating devices (FADs). Marine Biology, 159: 907–914.

Robert, M., Dagorn, L., Lopez, J., Moreno, G., and Deneubourg, J. L. 2013. Does social behavior influence the dynamics of aggregations formed by tropical tunas around floating objects? An experimental approach. Journal of Experimental Marine Biology and Ecology, 440: 238–243.

Rodriguez-Tress, P., Capello, M., Forget, F., Soria, M., Beeharry, S., Dussooa, N., and Dagorn, L. 2017. Associative behavior of yellowfin Thunnus albacares, skipjack Katsuwonus pelamis, and bigeye tuna T. obesus at anchored fish aggregating devices (FADs) off the coast of Mauritius. Marine Ecology Progress Series, 570: 213–222. http://www.int-res.com/abstracts/meps/v570/p213-222/.

Santiago, J., Uranga, J., Quincoces, I., Orue, B., Merino, G., Murua, H., and Boyra, G. 2020. A novel index of abundance of juvenile yellowfin tuna in the Atlantic Ocean derived from echosounder buoys. Collect. Vol. Sci. Pap. ICCAT, 76: 321–343.

Tolotti, M. T., Forget, F., Capello, M., Filmalter, J. D., Hutchinson, M., Itano, D., Holland, K., *et al.* 2020. Association dynamics of tuna and purse seine bycatch species with drifting fish aggregating devices (FADs) in the tropical eastern Atlantic Ocean. Fisheries Research, 226: 105521. Elsevier. https://doi.org/10.1016/j.fishres.2020.105521.

**Table 1:** Number of fishing sets and buoys used to estimate the average biomasse of skipjack tuna and the proportions of floating objects with tuna aggregations, respectively. The "FOB sets" column indicates the total number of fishing sets on floating objects (FOBs) from the logbook data corrected with the T3 process. The "sampled FOB sets" column indicates the number of sampled fishing sets used to estimate the species compositions and occurrences in associated FOB aggregations. "M3I buoy count" and "Total buoy count" represent the daily average number of French M3I buoys and total number of French buoys in the study area by quarter.

| Year | Quarter | FOB sets | Sampled FOB sets | M3I Buoy Count | Total buoy count |
|---|---|---|---|---|---|
| 2013 | Q1 | 171 | 49 | 329 | 333 |
| 2013 | Q2 | 247 | 88 | 349 | 363 |
| 2013 | Q3 | 406 | 112 | 496 | 550 |
| 2013 | Q4 | 505 | 155 | 377 | 509 |
| 2014 | Q1 | 321 | 78 | 328 | 578 |
| 2014 | Q2 | 229 | 54 | 451 | 831 |
| 2014 | Q3 | 472 | 130 | 517 | 927 |
| 2014 | Q4 | 405 | 85 | 666 | 1102 |
| 2015 | Q1 | 139 | 19 | 633 | 927 |
| 2015 | Q2 | 154 | 16 | 1000 | 1338 |
| 2015 | Q3 | 360 | 70 | 1335 | 1620 |
| 2015 | Q4 | 476 | 91 | 1498 | 1738 |
| 2016 | Q1 | 334 | 67 | 1718 | 1941 |
| 2016 | Q2 | 279 | 34 | 1710 | 1876 |
| 2016 | Q3 | 531 | 116 | 1414 | 1541 |
| 2016 | Q4 | 507 | 104 | 1376 | 1468 |
| 2017 | Q1 | 283 | 32 | 2069 | 2223 |
| 2017 | Q2 | 402 | 93 | 1717 | 2324 |
| 2017 | Q3 | 529 | 132 | 2022 | 2841 |
| 2017 | Q4 | 424 | 130 | 1925 | 2528 |
| 2018 | Q1 | 547 | 143 | 1911 | 2366 |
| 2018 | Q2 | 427 | 150 | 2004 | 2494 |
| 2018 | Q3 | 539 | 200 | 2064 | 2690 |
| 2018 | Q4 | 506 | 193 | 2184 | 2866 |
| 2019 | Q1 | 426 | 138 | 1980 | 2807 |
| 2019 | Q2 | 217 | 45 | 1780 | 2485 |
| 2019 | Q3 | 428 | 97 | 1783 | 2507 |
| 2019 | Q4 | 589 | 165 | 1722 | 2589 |
| 2020 | Q1 | 594 | 143 | 1508 | 2447 |
| 2020 | Q4 | 444 | 36 | 903 | 1630 |
| 2021 | Q1 | 359 | 65 | 758 | 1411 |
| 2021 | Q2 | 442 | 139 | 686 | 1571 |
| 2021 | Q3 | 430 | 111 | 775 | 1854 |
| 2021 | Q4 | 519 | 44 | 517 | 1421 |

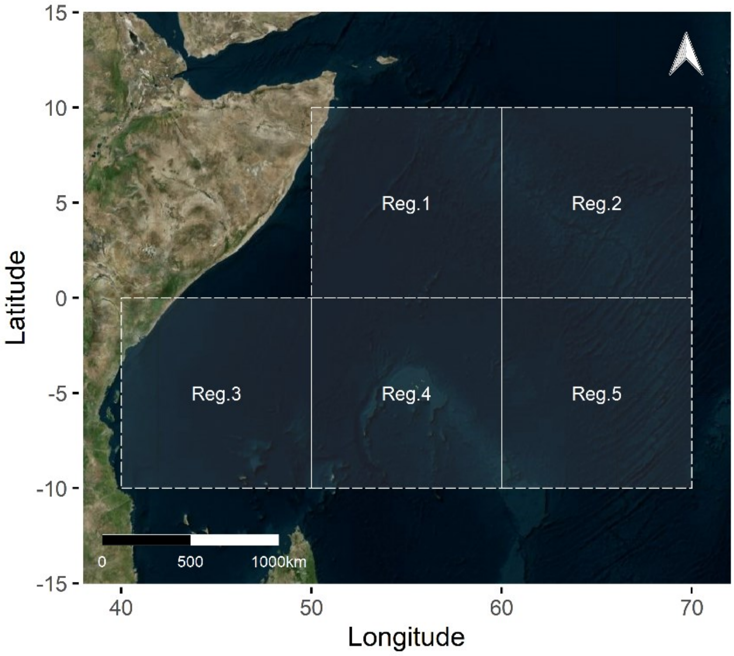


**Figure 1:** Spatial stratification of the study area

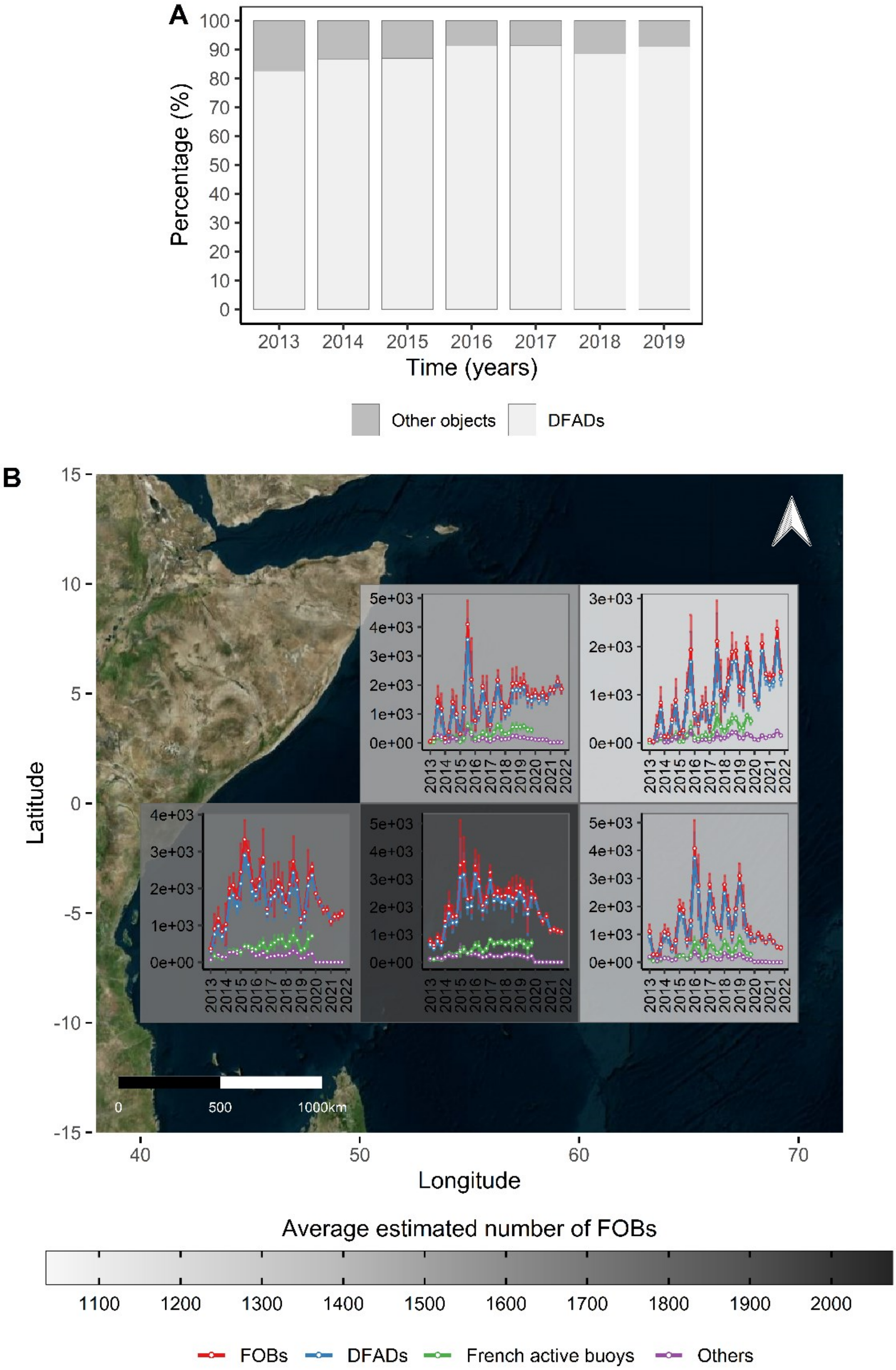


**Figure 2:** Estimates of the number of floating objects in the study area. (**a**), Percentage of drifting fish aggregating devices (DFADs) and other types of natural and artificial objects (Other objects, also referred to as LOGs in the text) reported by observers on board French tuna purse-seiners. (**b**) Quarterly averages of the daily number of active buoys in the French fleet, the estimated numbers of drifting fish aggregating devices (DFADs), the other objects (Others, also referred to as LOGs in the text), and the estimated total number of floating objects (FOBs =

DFADs + LOGs) by 10° × 10° spatial strata in the western Indian Ocean. The background colors indicate the average number of FOBs calculated from 2013 to 2021 in each spatial stratum.

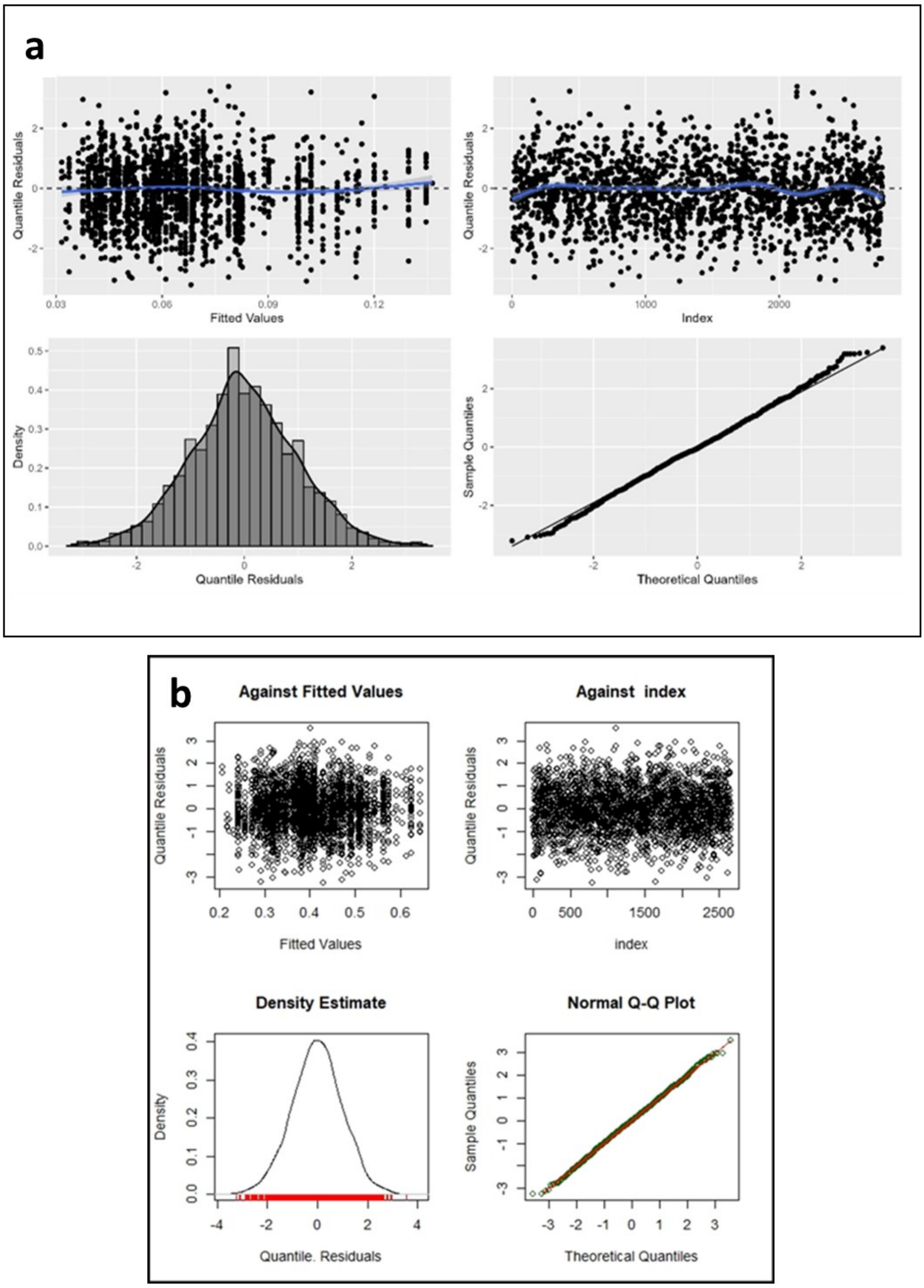


**Figure 3:** Residual diagnostic figures. (**a**) Zero and one-inflated beta models used to estimate missing composition values for skipjack tuna, (**b**) Binomial model used to estimate missing occurrence values for skipjack tuna.

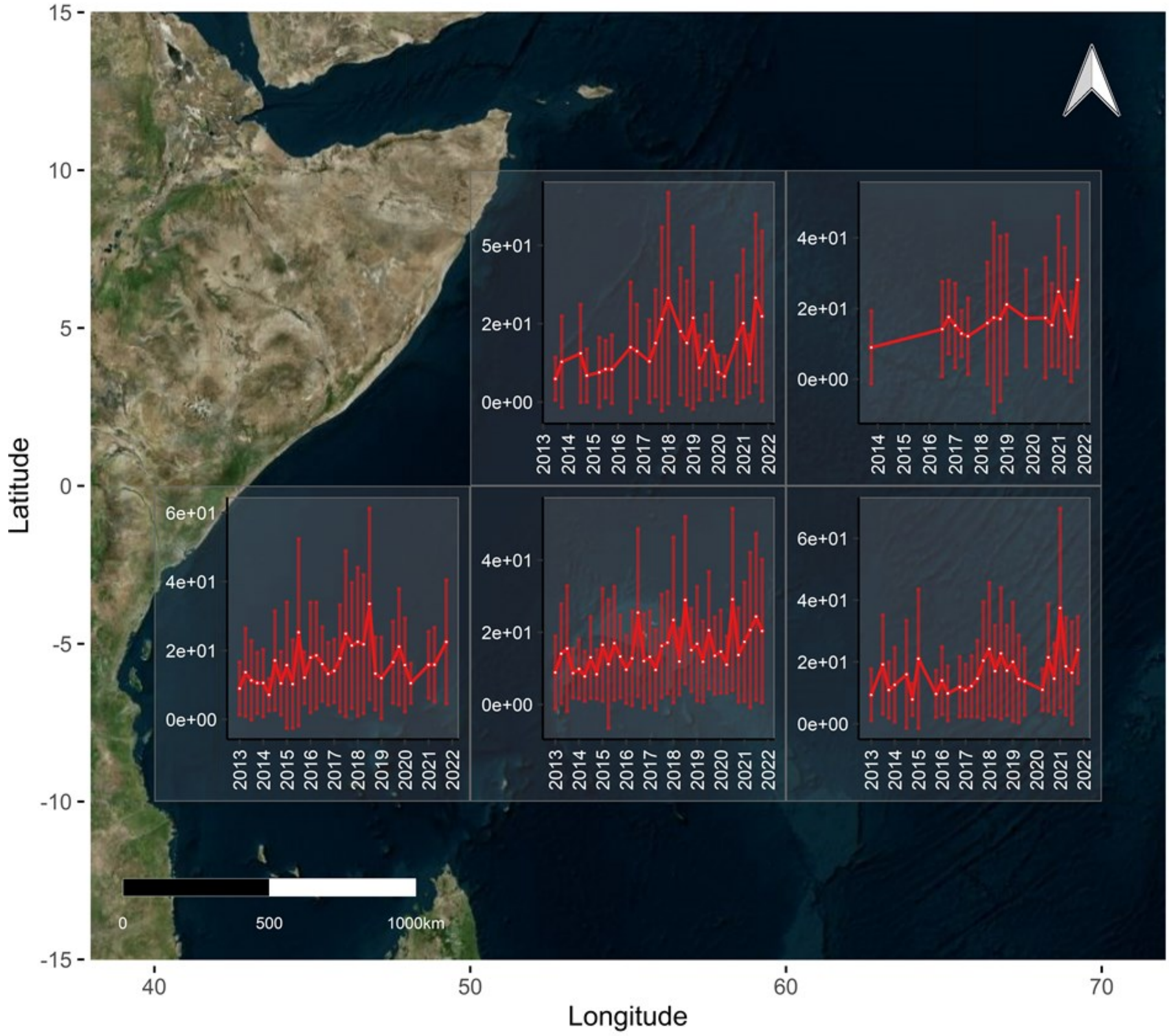


**Figure 4:** Quarterly averages of FOB-associated biomasses (in tonnes) skipjack tuna per FOB set by 10° × 10° spatial strata in the western Indian Ocean. The background colors indicate the average biomass calculated from 2013 to 2019 in each spatial stratum.

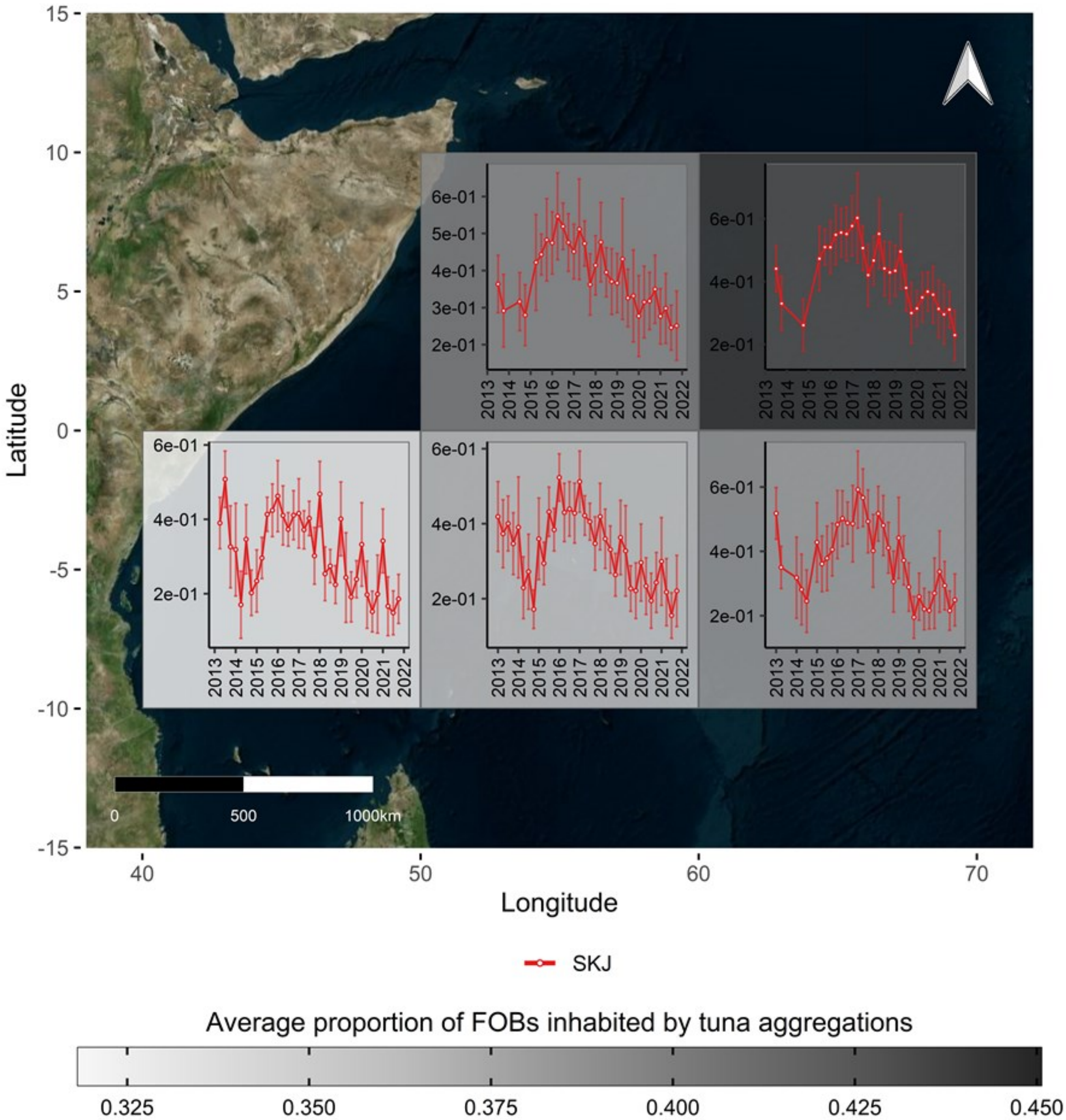


**Figure 5:** Quarterly averages of the daily proportion of FOBs inhabited by skipjack tuna by 10°×10° spatial strata in the western Indian Ocean. The background colors indicate the average proportion of FOBs with tuna aggregations greater than 1 tonne (all three species) from 2013 to 2019 in each spatial stratum.

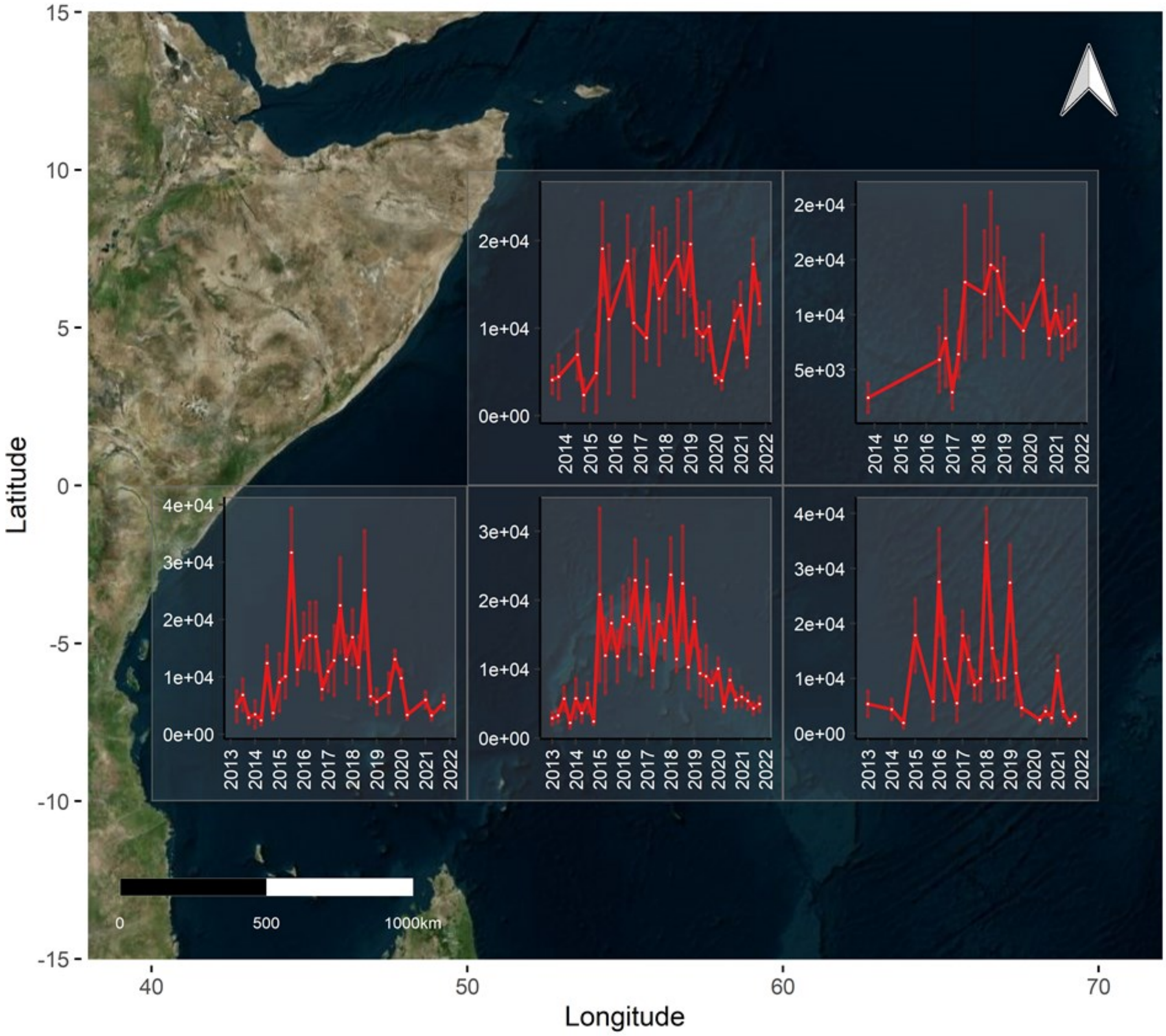


**Figure 6:** Quarterly estimates of the abundance of the associated component of skipjack tuna population by 10° × 10° spatial strata in the western Indian Ocean.

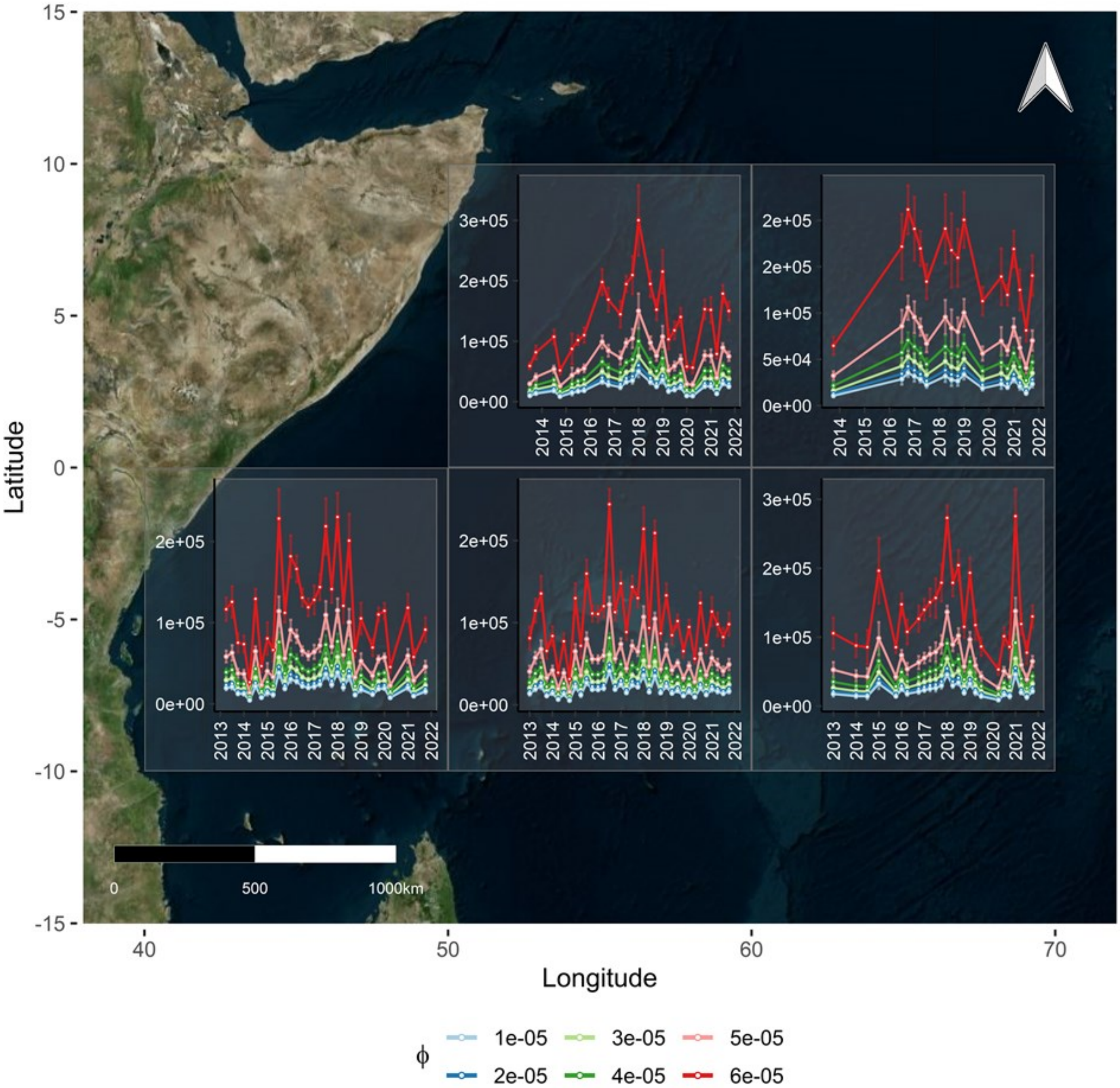


**Figure 7:** Quarterly estimates of the abundance of the free-swimming component of skipjack tuna population by 10° × 10° spatial strata in the western Indian Ocean.

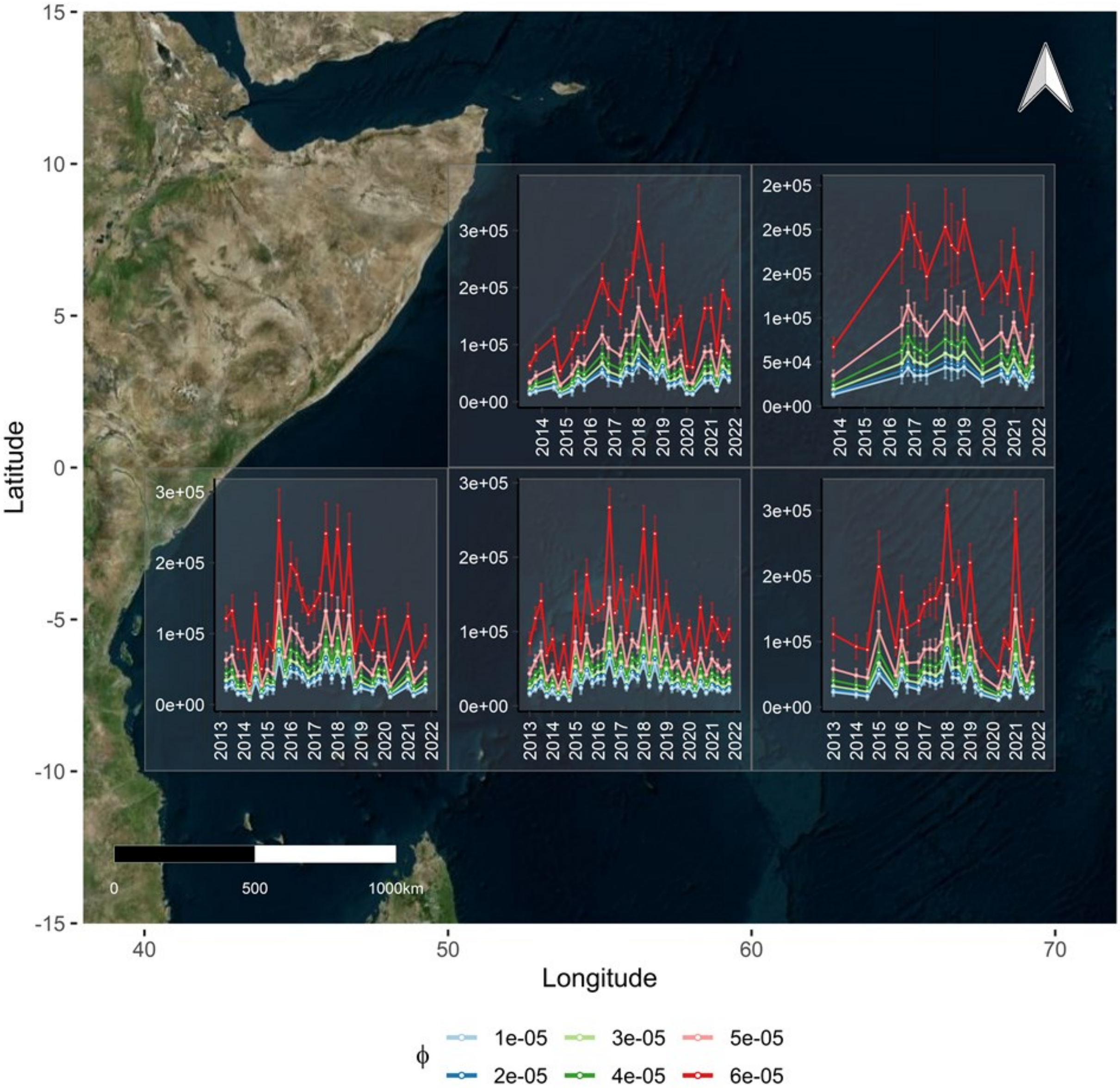


**Figure 8:** Quarterly estimates of the abundance of the skipjack tuna population by 10° × 10° spatial strata in the western Indian Ocean.

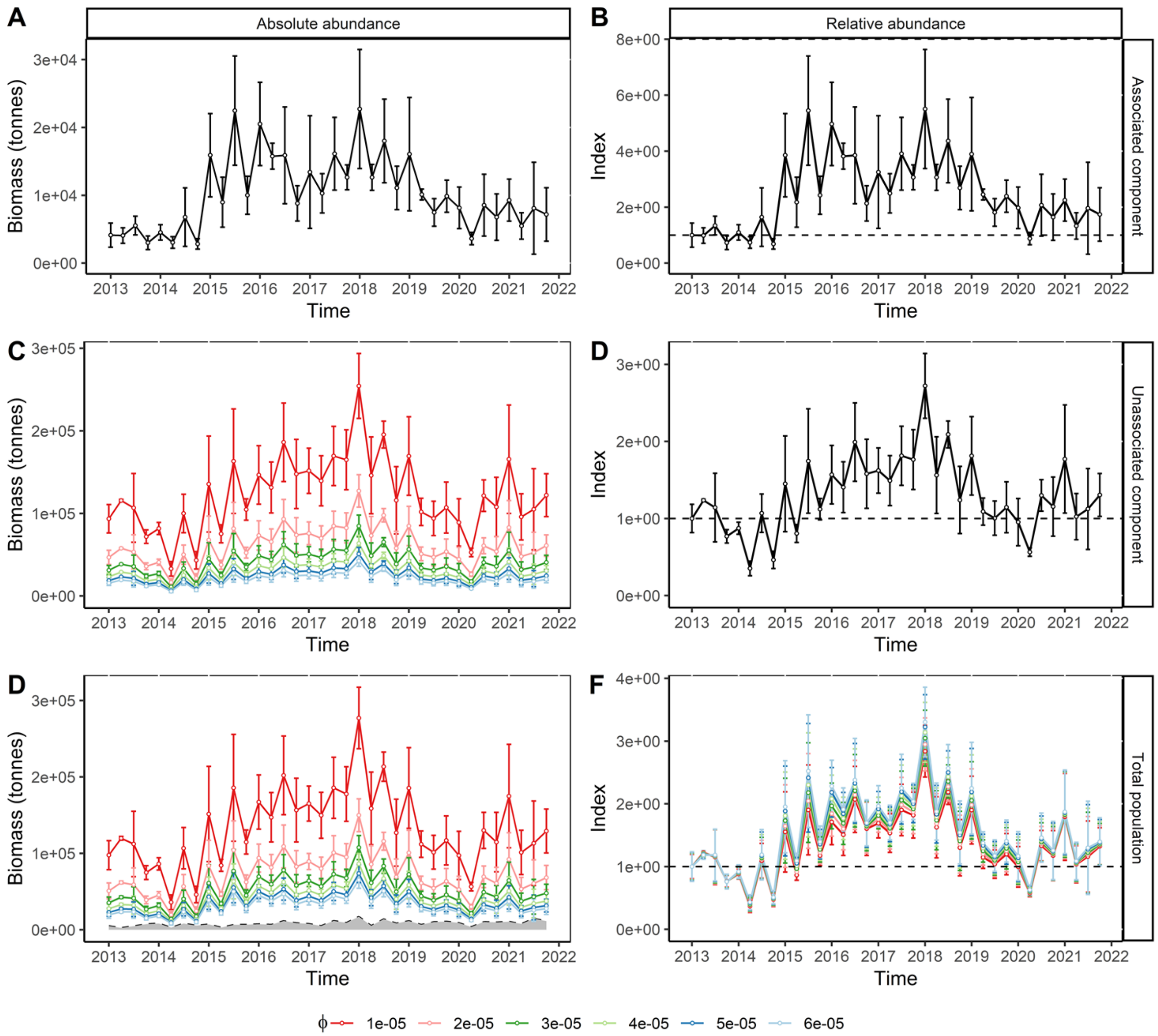


**Figure 9**: Abundance estimates from the Associative Behavior Based abundance Index (ABBI) for the different population component (associated and unassociated) of skipjack tuna in the western Indian Ocean. (A) Absolute and (B) relative abundance estimates of the associated component. (C) Absolute and (E) relative abundance estimates of the unassociated component. (E) Absolute and (F) relative abundance estimates of the total skipjack population